Doubly-Selective Channel Estimation in FBMC-OQAM and OFDM Systems

Ronald Nissel, Fjolla Ademaj[†‡], and Markus Rupp[‡]
[†] Christian Doppler Laboratory for Dependable Wireless Connectivity for the Society in Motion,
[‡] Institute of Telecommunications, TU Wien, Vienna, Austria
Email: ronald.nissel@gmail.com, {fademaj, mrupp}@nt.tuwien.ac.at

***Abstract*—We propose a method to estimate doubly-selective channels based on the time and frequency correlation of scattered pilots. To reduce the interference at the pilot and data positions, we apply an iterative interference cancellation scheme. Our method is applicable to arbitrary linear modulation techniques, with Orthogonal Frequency Division Multiplexing (OFDM) and Filter Bank Multicarrier Modulation (FBMC), being special cases. Simulations over doubly-selective channels show that our channel estimation method comes close to having perfect channel knowledge available. A downloadable Matlab code supports reproducibility.**

***Index Terms*—FBMC-OQAM, OFDM, Multipath channels, Time-varying channels, Channel Estimation.**

I. Introduction

Orthogonal Frequency Division Multiplexing (OFDM) is the dominant transmission technique of current wireless systems and is intended to remain relevant even in the next generation of wireless system (5G). However, the interest in alternative schemes, such as Filter Bank Multicarrier Modulation (FBMC) with Offset Quadrature Amplitude Modulation (OQAM), increased in recent years [1], [2]. FBMC has much better spectral properties when compared with OFDM, but also some additional disadvantages, such as a lower compatibility to Multiple-Input and Multiple-Output (MIMO) [3]–[5]. Moreover, all multi-carrier schemes have the drawback of a high Peak-to-Average Power Ratio (PAPR). Thus, additional processing might be necessary [6]. On the other hand, one of the biggest advantages of multi-carrier systems is that the transmission over a time-variant multi-path channel can often be modeled by one-tap channels, greatly simplifying the equalization. This works as long as the delay spread and the Doppler spread are sufficiently low [7]. Such condition, however, is not always fulfilled. In highly doubly-selective channels, symbols interfere with each other. Channel estimation and equalization then becomes more challenging.

To estimate doubly-selective channels, authors in [8] and [9] utilize a Minimum Mean Squared Error (MMSE) channel estimation method, but consider only one OFDM symbol in time. This requires clustered pilots. MMSE channel estimation was also investigated in FBMC [10], but the authors ignore the time-varying nature of wireless channels. Many other authors employ a basis expansion model [11], [12] to estimate doubly-selective channels. Here, the time variation is modeled by a basis expansion, for example, an exponential basis [13], a polynomial basis [14], a Slepian basis [15] or an MMSE interpolation basis [16]. Some authors argue that statistical models are bulky and difficult to handle [11], which is also the main reason why they employ a basis expansion model. However, we utilize a compact matrix description, allowing to easily incorporate channel statistics, so that all elements of a doubly-selective channel can be accurately estimated with just a few pilots. The novel contributions of our paper can be summarized as follows:

1) We propose a doubly-selective channel estimation method that does not require clustered pilots or a basis expansion model.
2) We generalize our previous paper, see [17], so that our method is not only applicable to OFDM, as in [17], but to arbitrary linear modulation methods, including FBMC.
3) In contrast to [17], we employ a low-complexity interference cancellation scheme instead of a computationally demanding MMSE equalization.

To support reproducibility, our Matlab code can be downloaded at **https://github.com/rnissel/Channel-Estimation.**

II. System Model

In multi-carrier systems, the transmitted symbols $x_{l,k}$, at subcarrier position l and time position k, are modulated by the basis pulses $g_{l,k}(t)$, so that the transmitted signal in the time domain, $s(t)$, becomes [1], [2],

$$s(t) = \sum_{k=0}^{K-1} \sum_{l=0}^{L-1} g_{l,k}(t)\, x_{l,k}, \tag{1}$$

with

$$g_{l,k}(t) = p_{\mathrm{TX}}(t-kT)\ \mathrm{e}^{\mathrm{j}2\pi\, lF\,(t-kT)}\ \mathrm{e}^{\mathrm{j}\theta_{l,k}}. \tag{2}$$

Basis pulse $g_{l,k}(t)$ is nothing else than a time and frequency shifted version of prototype filter $p_{\mathrm{TX}}(t)$. At the receiver, a different prototype filter might be used, so that the received basis pulses $q_{l,k}(t)$ can be expressed as,

$$q_{l,k}(t) = p_{\mathrm{RX}}(t-kT)\ \mathrm{e}^{\mathrm{j}2\pi\, lF\,(t-kT)}\ \mathrm{e}^{\mathrm{j}\theta_{l,k}}. \tag{3}$$

In Cyclic Prefix (CP)-OFDM, $p_{\mathrm{TX}}(t)$ is a rectangular pulse and $p_{\mathrm{RX}}(t)$ a slightly shorter rectangular pulse. Furthermore, the time-frequency spacing is $TF = 1 + T_{\mathrm{CP}}F$ and the basis pulses are orthogonal, that is, $\langle g_{l_1,k_1}(t), q_{l_2,k_2}(t)\rangle = \delta_{(l_1-l_2),(k_1-k_2)}$. In FBMC, on the other hand, $p(t) =$

$p_{\mathrm{TX}}(t) = p_{\mathrm{RX}}(t)$ is a smoother function, for example based on a Hermite prototype filter [1], and (complex) orthogonal for a time-frequency spacing of $TF = 2$. To improve the spectral efficiency in FBMC, the time-frequency spacing is reduced to $TF = 0.5$, and only real-valued data symbols $x_{l,k} \in \mathbb{R}$ are transmitted. Orthogonality then only holds in the real domain, $\Re\{\langle g_{l_1,k_1}(t), q_{l_2,k_2}(t)\rangle\} = \delta_{(l_1-l_2),(k_1-k_2)}$.

To simplify the analytical description, we consider a discrete time system model [1], where we sample the transmitted basis pulses in (2) with rate $f_{\mathrm{s}} = 1/\Delta t = F N_{\mathrm{FFT}}$ and stack all samples in a large vector $\mathbf{g}_{l,k} \in \mathbb{C}^{N\times 1}$. Additionally, we stack all basis pulse vectors in matrix $\mathbf{G} = \begin{bmatrix}\mathbf{g}_{0,0} & \cdots & \mathbf{g}_{L-1,K-1}\end{bmatrix} \in \mathbb{C}^{N\times LK}$. In a similar way, we stack the receive basis pulse samples, see (2), in matrix $\mathbf{Q} = \begin{bmatrix}\mathbf{q}_{0,0} & \cdots & \mathbf{q}_{L-1,K-1}\end{bmatrix} \in \mathbb{C}^{N\times LK}$. Note that in OFDM, the orthogonality condition implies that $\mathbf{Q}^{\mathsf{H}}\mathbf{G} = \mathbf{I}_{LK}$, while in FBMC only the real orthogonality condition holds true, that is, $\Re\{\mathbf{Q}^{\mathsf{H}}\mathbf{G}\} = \mathbf{I}_{LK}$.

The transmission over a doubly-selective channel is described by the following input-output relationship [1],

$$\mathbf{y} = \mathbf{D}\,\mathbf{x} + \mathbf{n}, \tag{4}$$

where $\mathbf{x} = \begin{bmatrix}x_{0,0} & \cdots & x_{L-1,K-1}\end{bmatrix} \in \mathbb{C}^{LK\times 1}$ represents the transmitted data symbols in vectorized form, $\mathbf{y} \in \mathbb{C}^{LK\times 1}$ the received symbols, $\mathbf{n} \sim \mathcal{CN}(\mathbf{0}, P_{\mathrm{n}}\,\mathbf{Q}^{\mathsf{H}}\mathbf{Q})$ the Gaussian noise, and $\mathbf{D} \in \mathbb{C}^{LK\times LK}$ the transmission matrix, defined as,

$$\mathbf{D} = \mathbf{Q}^{\mathsf{H}}\,\mathbf{H}\,\mathbf{G}. \tag{5}$$

The time-variant channel in (5) is described by a time-variant convolution matrix $\mathbf{H} \in \mathbb{C}^{N\times N}$, where $[\mathbf{H}]_{n,j} = h_{\mathrm{conv.}}[n, n-j]$, with $h_{\mathrm{conv.}}[n, m_\tau]$ denoting the time-variant impulse response. If the delay spread and the Doppler spread are sufficiently low, the off-diagonal elements of $\mathbf{D}$ can be neglected, allowing us to approximate the transmission matrix by $\mathbf{D} \approx \mathrm{diag}\{\mathbf{h}\}\mathbf{Q}^{\mathsf{H}}\mathbf{G}$, with one-tap channel $\mathbf{h} \in \mathbb{C}^{LK\times 1}$. The $l + Lk$-th element of $\mathbf{h}$ is given by $h_{l,k} = \mathbf{q}_{l,k}^{\mathsf{H}}\mathbf{H}\,\mathbf{g}_{l,k}$ and can interpreted as the "sampled" time-variant transfer function at frequency lF and time kT.

III. LS Channel Estimation

We consider pilot symbol aided channel estimation [18], [19], that is, a total of $|\mathcal{P}|$ "data" symbols, $\mathbf{x}_{\mathcal{P}} \in \mathbb{C}^{|\mathcal{P}|\times 1}$, the so-called pilots, are known a priori at the receiver. This allows a Least Squares (LS) estimation of the one-tap channel at the pilot positions, $\hat{\mathbf{h}}_{\mathcal{P}}^{\mathrm{LS}} \in \mathbb{C}^{|\mathcal{P}|\times 1}$, according to,

$$\hat{\mathbf{h}}_{\mathcal{P}}^{\mathrm{LS}} = \mathrm{diag}\{\mathbf{x}_{\mathcal{P}}\}^{-1}\,\mathbf{y}_{\mathcal{P}}. \tag{6}$$

Unfortunately, the imaginary interference in FBMC prevents a straightforward LS estimation of the one-tap channel. Additional preprocessing becomes necessary [20]–[25]. To be specific, we apply precoding by,

$$\mathbf{x} = \mathbf{C}\,\tilde{\mathbf{x}}, \tag{7}$$

where $\tilde{\mathbf{x}}$ denotes the data symbols and $\mathbf{C}$ cancels the imaginary interference at the pilot positions, that is,

$$\Im\{\mathbf{q}_{\mathcal{P}}^{\mathsf{H}}\mathbf{G}\}\mathbf{C}\,\tilde{\mathbf{x}} = \mathbf{0}, \tag{8}$$

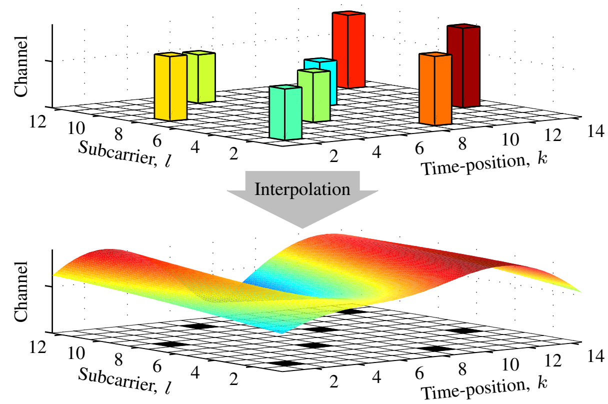

Fig. 1. The LS channel estimates at the pilot positions are interpolated to estimate the time-variant transfer function. Note that the elements of transmission matrix $\mathbf{D}$ can be directly estimated without the detour of the time-variant transfer function, see (9).

see [21], [22] for more details. Note that cancelation matrix $\mathbf{C}$ may represent the auxiliary symbol method [22] or the data spreading approach [21]. The latter requires additional despreading at the receiver.

IV. Doubly Selective Channel Estimation

In case of a doubly-selective channel, many papers [16], [26], try to estimate the channel impulse response, that is, $\hat{\mathbf{H}}$. However, estimating the impulse response is quite problematic because in practical systems the number of active subcarriers is always lower than the Fast Fourier Transform (FFT) size, that is, $L < N_{\mathrm{FFT}}$. This implies that the channel transfer function at the zero subcarriers cannot be accurately estimated, preventing also an accurate estimation of the impulse response. By applying an inverse Fourier transform onto the channel transfer function of the L active subcarriers, one only obtains a pseudo impulse response, implicitly assuming a rectangular filter. In particular, the delay taps of the pseudo impulse response are no longer limited in time (within the symbol duration), even though the true impulse response might be. This is caused by the discontinuity of the channel transfer function at the edge subcarriers and becomes problematic for estimation methods which rely on the assumption that the delay taps are limited in time. Another aspect is the computational complexity. Even if one is able to accurately estimate the impulse response, the matrix multiplication in (5) still needs to be evaluated, implying a huge computational burden. All those drawbacks can be avoided by directly estimating transmission matrix $\hat{\mathbf{D}}$. To some extend, this is already happening in practical systems, as the one-tap channel is usually estimated through interpolation. Those one-tap channel coefficients correspond to the diagonal elements of $\hat{\mathbf{D}}$.

The main idea of our channel estimation method is illustrated in Figure 1. The "sampled" time-variant transfer function (at the pilot positions) is interpolated, delivering an estimate of the full time-variant transfer function. This is possible because of a high correlation in time and frequency.

As already mentioned before, it is computationally more efficient to directly estimate $\hat{\mathbf{D}}$ without the detour of the channel transfer function, whereby the underlying correlation is preserved. One element of transmission matrix $\hat{\mathbf{D}}$, at row position $\overline{l_1 k_1} = l_1 + L k_1$ and column position $\overline{l_2 k_2} = l_2 + L k_2$, can then be estimated by

$$[\hat{\mathbf{D}}]_{\overline{l_1 k_1}, \overline{l_2 k_2}} = \tilde{\mathbf{w}}_{l_1,k_1,l_2,k_2}^{\mathsf{H}} \, \hat{\mathbf{h}}_{\mathcal{P}}^{\mathrm{LS}}, \tag{9}$$

where $\tilde{\mathbf{w}}_{l_1,k_1,l_2,k_2} \in \mathbb{C}^{|\mathcal{P}| \times 1}$ represents a weighting vector and $\hat{\mathbf{h}}_{\mathcal{P}}^{\mathrm{LS}} \in \mathbb{C}^{|\mathcal{P}| \times 1}$ the LS channel estimates at the pilot positions, see (6). The weighting vector has a major influence on the channel estimation accuracy. We consider an MMSE weighting vector, the best possible channel estimation method in terms of MSE. By utilizing the orthogonal projection theorem,

$$\mathbb{E}\left\{ \left([\mathbf{D}]_{\overline{l_1 k_1}, \overline{l_2 k_2}} - [\hat{\mathbf{D}}]_{\overline{l_1 k_1}, \overline{l_2 k_2}} \right) [\hat{\mathbf{D}}]_{\overline{l_1 k_1}, \overline{l_2 k_2}}^{\mathsf{H}} \right\} = 0, \tag{10}$$

which states that the error of the estimator must be orthogonal to the estimator, the MMSE weighting vector in (9) can be calculated by,

$$\tilde{\mathbf{w}}_{l_1,k_1,l_2,k_2} = \mathbf{R}_{\hat{\mathbf{h}}_{\mathcal{P}}^{\mathrm{LS}}}^{-1} \, \mathbf{r}_{\hat{\mathbf{h}}_{\mathcal{P}}^{\mathrm{LS}}, [\mathbf{D}]_{\overline{l_1 k_1}, \overline{l_2 k_2}}}, \tag{11}$$

with $\mathbf{R}_{\hat{\mathbf{h}}_{\mathcal{P}}^{\mathrm{LS}}} = \mathbb{E}\{\hat{\mathbf{h}}_{\mathcal{P}}^{\mathrm{LS}} (\hat{\mathbf{h}}_{\mathcal{P}}^{\mathrm{LS}})^{\mathsf{H}}\} \in \mathbb{C}^{|\mathcal{P}| \times |\mathcal{P}|}$ denoting the correlation matrix of the LS channel estimates at the pilot positions and $\mathbf{r}_{\hat{\mathbf{h}}_{\mathcal{P}}^{\mathrm{LS}}, [\mathbf{D}]_{\overline{l_1 k_1}, \overline{l_2 k_2}}} \in \mathbb{C}^{|\mathcal{P}| \times 1}$ the correlation vector between the LS channel estimates at the pilot positions and one element of transmission matrix $\mathbf{D}$. Very often, the biggest challenge is to find the required correlation matrices. Thanks to our matrix notation, however, finding those matrices is relatively easy. Let us first consider the correlation between the i-th LS channel estimate and the j-th LS channel estimate, $\mathbf{R}_{\hat{h}_{\mathcal{P}_i}^{\mathrm{LS}}, \hat{h}_{\mathcal{P}_j}^{\mathrm{LS}}} = \mathbb{E}\{\hat{h}_{\mathcal{P}_i}^{\mathrm{LS}} (\hat{h}_{\mathcal{P}_j}^{\mathrm{LS}})^{\mathsf{H}}\} \in \mathbb{C}^{1 \times 1}$. Assuming $i \neq j$, the interference as well as the noise are uncorrelated, so that $\mathbf{R}_{\hat{h}_{\mathcal{P}_i}^{\mathrm{LS}}, \hat{h}_{\mathcal{P}_j}^{\mathrm{LS}}} = \mathbf{R}_{h_{\mathcal{P}_i}, h_{\mathcal{P}_j}}$. By utilizing the Kronecker product, $h_{\mathcal{P}_i} = \mathbf{q}_{\mathcal{P}_i}^{\mathsf{H}} \mathbf{H} \, \mathbf{g}_{\mathcal{P}_i} = \left(\mathbf{g}_{\mathcal{P}_i}^{\mathsf{T}} \otimes \mathbf{q}_{\mathcal{P}_i}^{\mathsf{H}} \right) \mathrm{vec}\{\mathbf{H}\}$, we calculate the correlation between the LS channel estimates at the pilot positions, $i \neq j$, according to,

$$\mathbf{R}_{\hat{h}_{\mathcal{P}_i}^{\mathrm{LS}}, \hat{h}_{\mathcal{P}_j}^{\mathrm{LS}}} = \left(\mathbf{g}_{\mathcal{P}_i}^{\mathsf{T}} \otimes \mathbf{q}_{\mathcal{P}_i}^{\mathsf{H}} \right) \mathbf{R}_{\mathrm{vec}\{\mathbf{H}\}} \left(\mathbf{g}_{\mathcal{P}_j}^{\mathsf{T}} \otimes \mathbf{q}_{\mathcal{P}_j}^{\mathsf{H}} \right)^{\mathsf{H}}. \tag{12}$$

For the power at the pilot positions, we have to consider interference $\mathbf{g}_{\mathcal{P}_i}^{\mathsf{T}} \rightarrow \mathbf{C}^{\mathsf{T}} \mathbf{G}^{\mathsf{T}}$ and noise $P_{\mathrm{n}} \mathbf{q}_{\mathcal{P}_i}^{\mathsf{H}} \mathbf{q}_{\mathcal{P}_i}$, leading to

$$\mathbf{R}_{\hat{h}_{\mathcal{P}_i}^{\mathrm{LS}}} = \frac{\mathrm{tr}\left\{ \left(\mathbf{C}^{\mathsf{T}} \mathbf{G}^{\mathsf{T}} \otimes \mathbf{q}_{\mathcal{P}_i}^{\mathsf{H}} \right) \mathbf{R}_{\mathrm{vec}\{\mathbf{H}\}} \left(\mathbf{C}^{\mathsf{T}} \mathbf{G}^{\mathsf{T}} \otimes \mathbf{q}_{\mathcal{P}_i}^{\mathsf{H}} \right)^{\mathsf{H}} \right\} + P_{\mathrm{n}} \mathbf{q}_{\mathcal{P}_i}^{\mathsf{H}} \mathbf{q}_{\mathcal{P}_i}}{P_{\mathcal{P}}}. \tag{13}$$

The cross-correlation in (12) and the auto-correlation in (13) build up the overall correlation matrix $\mathbf{R}_{\hat{\mathbf{h}}_{\mathcal{P}}^{\mathrm{LS}}} \in \mathbb{C}^{|\mathcal{P}| \times |\mathcal{P}|}$, and depend on the correlation matrix of the vectorized channel, $\mathbf{R}_{\mathrm{vec}\{\mathbf{H}\}} = \mathbb{E}\{\mathrm{vec}\{\mathbf{H}\} \mathrm{vec}\{\mathbf{H}\}^{\mathsf{H}}\}$. The elements of this correlation matrix can easily be calculated because they are just the correlation of the time-variant impulse response, that is, $\mathbb{E}\{h_{\mathrm{conv.}}[n_1, m_1] \, h_{\mathrm{conv.}}^*[n_2, m_2]\}$, assumed to be perfectly known. Only the mapping of this correlation to the correct position in $\mathbf{R}_{\mathrm{vec}\{\mathbf{H}\}}$ is a bit challenging because of the vectorized structure. Similar as in (12), the correlation between the LS channel estimate at the i-th pilot position and one element of transmission matrix $\mathbf{D}$ can be calculated by,

$$\mathbf{r}_{\hat{h}_{\mathcal{P}_i}^{\mathrm{LS}}, [\mathbf{D}]_{\overline{l_1 k_1}, \overline{l_2 k_2}}} = \left(\mathbf{g}_{\mathcal{P}_i}^{\mathsf{T}} \otimes \mathbf{q}_{\mathcal{P}_i}^{\mathsf{H}} \right) \mathbf{R}_{\mathrm{vec}\{\mathbf{H}\}} \left(\mathbf{g}_{l_2,k_2}^{\mathsf{T}} \otimes \mathbf{q}_{l_1,k_1}^{\mathsf{H}} \right)^{\mathsf{H}}, \tag{14}$$

and builds up correlation vector $\mathbf{r}_{\hat{\mathbf{h}}_{\mathcal{P}}^{\mathrm{LS}}, [\mathbf{D}]_{\overline{l_1 k_1}, \overline{l_2 k_2}}} \in \mathbb{C}^{|\mathcal{P}| \times 1}$. With (12)-(14) we have all the necessary tools to calculate the MMSE weighting vector in (11), that is, $\tilde{\mathbf{w}}_{l_1,k_1,l_2,k_2}$. One might think that our channel estimation method is unrealistic because the correlation matrices are not perfectly known in practical systems. While it is indeed hard to find the true correlation matrices, a rough approximation can easily be found and is often sufficient. For example, in the context of OFDM, testbed measurements at 400 km/h have already validated that our MMSE channel estimation works in real world testbed scenarios [17]. To measure at such high velocities, we augmented the Vienna Wireless Testbed by a rotation wheel unit [27], [28]. The measurement results in [17] indicate that our channel estimation method, see (9) and (11), performs close to perfect channel knowledge. In [17] we considered MMSE equalization instead of a low-complexity interference cancellation scheme. Still, in contrast to many other works related to time-variant channel estimation, our MMSE channel estimation method was already proven to work in real world testbed scenarios, at least in the context of OFDM.

V. Interference Cancellation

Besides the challenge of doubly-selective channel estimation, channel equalization is equally important [29], [30], for which we consider a low-complexity interference cancellation scheme [31]. Interference cancellation is also important for the channel estimation process because the LS channel estimates at the pilot positions are corrupted by interference. By canceling this interference, the channel estimation accuracy can be improved. Our iterative channel estimation and interference cancellation scheme works as follows, where the superscript $(\cdot)^{(\mathrm{i})}$ denotes the i-th iteration step:

1) MMSE channel estimation of transmission matrix $\hat{\mathbf{D}}^{(0)}$, see (9) and (11).
2) One-tap equalization and quantization, $\hat{x}_{l,k}^{(0)} = \mathcal{Q}\left\{ y_{l,k}^{(0)} / \hat{h}_{l,k}^{(0)} \right\}$, with $\hat{\mathbf{h}}^{(0)} = \mathrm{diag}\{\hat{\mathbf{D}}^{(0)}\}$.
3) Initialize with $\mathrm{i} = 0$.
4) Interference cancellation, $\mathbf{y}^{(\mathrm{i}+1)} = \mathbf{y} - (\hat{\mathbf{D}}^{(\mathrm{i})} - \mathrm{diag}\{\mathrm{diag}\{\hat{\mathbf{D}}^{(\mathrm{i})}\}\}) \, \hat{\mathbf{x}}^{(\mathrm{i})}$
5) Improved estimation of transmission matrix $\hat{\mathbf{D}}^{(\mathrm{i}+1)}$, enabled by a reduced interference at the pilot positions.
6) Improved one-tap equalization and quantization $\hat{x}_{l,k}^{(\mathrm{i}+1)} = \mathcal{Q}\left\{ y_{l,k}^{(\mathrm{i}+1)} / \hat{h}_{l,k}^{(\mathrm{i}+1)} \right\}$
7) Repeat Step 4 to Step 7. We consider $\mathrm{i} = 0, 1, ..., 4$.

Note that the underlying correlation in (13) does not take interference cancellation at the pilot positions into account,

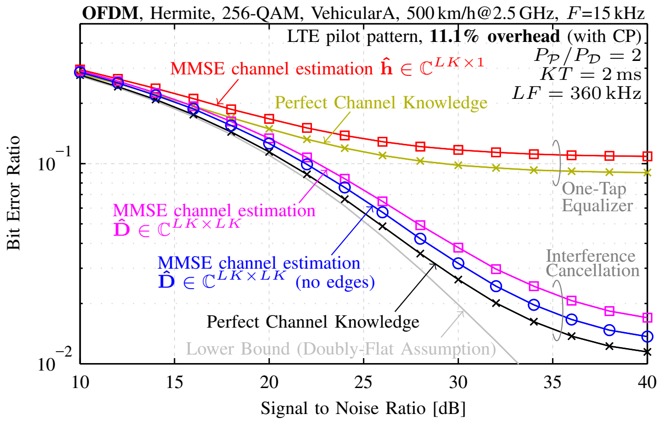

Fig. 2. Our proposed doubly-selective channel estimation method performs close to perfect channel knowledge.

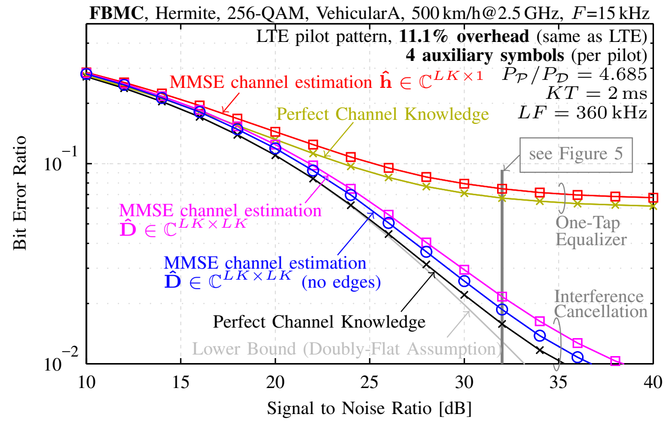

Fig. 3. Compared to Figure 2, the performance is better because the additional pilot symbol power is taken from the auxiliary symbols (which are close to zero) and not from the data symbols.

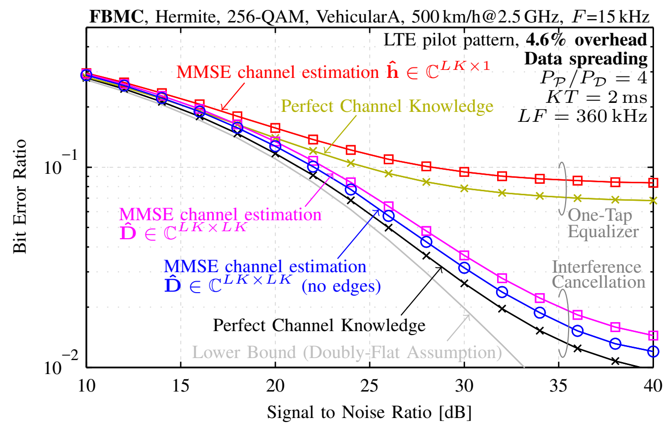

Fig. 4. Compared with Figure 3, the BER is slightly worse because of spreading and the fact that the additional pilot power is taken from the data symbols. However, the spreading method has a lower overhead and thus a higher data rate.

because nonlinearities make the analytical calculation challenging. To circumvent this problem, we employ a slightly mismatched MMSE estimation. For iteration step $\mathrm{i} = 0, 1, 2$, we consider the correlation as described in (13), while for iteration step $\mathrm{i} = 3$ and $\mathrm{i} = 4$, we assume that the interference is perfectly canceled, transforming matrix product $\mathbf{C}^\mathsf{T}\mathbf{G}^\mathsf{T}$ in (13) into $\mathbf{C}^\mathsf{T}\mathbf{G}^\mathsf{T} \rightarrow \sqrt{P_\mathcal{P}}\,\mathbf{g}_{\mathcal{P}_i}^\mathsf{T}$.

VI. Numerical Results

For our numerical evaluations, we consider a Long Term Evolution (LTE) like OFDM signal. We assume a diamond-shaped pilot pattern, same as in LTE, that is, $|\mathcal{P}| = 32$ pilots are distributed over a time-frequency resource of $KT = 2\,\mathrm{ms}$ and $LF = 360\,\mathrm{kHz}$, representing the transmission of two subframes with eight resource blocks in total. The overhead in OFDM, including pilot symbols and the CP, is $\frac{LF\,T_{\mathrm{CP}}K + |\mathcal{P}|}{KTLF} = 11.1\%$. Figure 2 shows the Bit Error Ratio (BER) over the Signal-to-Noise Ratio (SNR) for OFDM. Note that the BER is relatively high because of a 256-Quadrature Amplitude Modulation (QAM) signal constellation. To improve the channel estimation accuracy, we consider a pilot-to-data power offset of $P_\mathcal{P}/P_\mathcal{D} = 2$. A one-tap equalizer performs poorly once interference starts to dominate the noise. By employing our interference cancellation scheme, on the other hand, the performance can be significantly improved. Overall, our doubly-selective channel estimation technique performs close to perfect channel knowledge (only a small SNR shift of approximately 1 dB for the "no edges" curve). For the "no edges" MMSE channel estimation curve in Figure 2, we exclude time-frequency positions close to the edge, that is, we consider only points which are in the center of the frame. One can imagine a sliding block with an inner and an outer block where only the inner block is evaluated for the BER, while the outer block only contributes to the channel estimation. In Figure 2 we also include the lower bound of doubly-flat fading in combination with perfect channel knowledge and no pilot-to-data power offset.

Figure 3 shows the BER over SNR for FBMC, using the auxiliary symbol channel estimation method. We employ four auxiliary symbols per pilot, guaranteeing that the channel induced interference at the pilot position is relatively low. The overhead is the same as in LTE, that is, $\frac{TF(|\mathcal{P}|+|\mathcal{A}|)}{KTLF} = 11.1\%$. Furthermore, the auxiliary symbol power is close to zero, allowing us to increase the pilot-to-data power offset to 4.685. In contrast to OFDM, however, we do not lose any data symbol power, improving the performance further. Because we have in FBMC more power available for the data symbols than in OFDM, and because the channel induced interference is lower, FBMC shows a better BER performance than OFDM. Again, our MMSE channel estimation scheme performs close to perfect channel knowledge, showing its capability to deal with doubly-selective channels.

Figure 4 shows the BER for FBMC based on the data spreading approach, which has a relatively low overhead of $\frac{TF|\mathcal{P}|2}{KTLF} = 4.4\%$. Similar as in OFDM, we consider a pilot-to-data power offset of two (equal to four in the real domain) to improve the channel estimation accuracy. Again, our doubly-selective channel estimation method performs close to perfect channel knowledge. Compared to FBMC based on

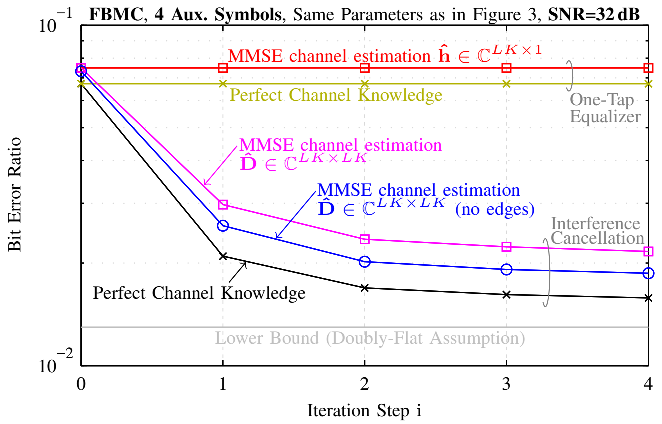

Fig. 5. We consider the same parameters as in Figure 3. The first iteration step, see Section V, greatly improves the BER, which soon saturates.

the auxiliary method, however, the performance is slightly worse because of the SNR shift. Additionally, we have to despread symbols, further reducing the BER performance when compared to the auxiliary symbol method. However, one has to keep in mind that the data rate is higher than for the auxiliary symbol method.

Finally, Figure 5 shows how the number of iteration steps, see Section V, improves the BER. We consider FBMC based on the auxiliary symbol method and an SNR of 32 dB. The first iteration step greatly improves the BER, which soon saturates.

VII. Conclusion

We have proposed a doubly-selective channel estimation and interference cancellation scheme. Our method is applicable to any linear modulation scheme, such as, OFDM and FBMC. FBMC based on the auxiliary symbol method outperforms OFDM in terms of BER. FBMC based on that data spreading method performs slightly worse than FBMC based on the auxiliary symbol method, but has the additional advantage of a higher data rate.

Acknowledgment: The financial support by the Austrian Federal Ministry of Science, Research and Economy, the National Foundation for Research, Technology and Development, and the TU Wien is gratefully acknowledged.

References

[1] R. Nissel, S. Schwarz, and M. Rupp, "Filter bank multicarrier modulation schemes for future mobile communications," *IEEE Journal on Selected Areas in Communications*, vol. 35, no. 8, pp. 1768–1782, 2017.
[2] R. Nissel, "Filter bank multicarrier modulation for future wireless systems," Dissertation, TU Wien, 2017. [Online]. Available: https://publik.tuwien.ac.at/files/publik_265168.pdf
[3] R. Nissel and M. Rupp, "Enabling low-complexity MIMO in FBMC-OQAM," in *IEEE Globecom Workshops (GC Wkshps)*, Dec 2016.
[4] R. Nissel, J. Blumenstein, and M. Rupp, "Block frequency spreading: A method for low-complexity MIMO in FBMC-OQAM," in *IEEE SPAWC*, July 2017.
[5] R. Nissel, E. Zöchmann, M. Lerch, S. Caban, and M. Rupp, "Low-latency MISO FBMC-OQAM: It works for millimeter waves!" in *IEEE International Microwave Symposium*, June 2017.
[6] R. Nissel and M. Rupp, "Pruned DFT spread FBMC: Low PAPR,low latency, high spectral efficiency," *IEEE Trans. Commun.*, 2018, to appear.
[7] R. Nissel and M. Rupp, "OFDM and FBMC-OQAM in doubly-selective channels: Calculating the bit error probability," *IEEE Communications Letters*, vol. 21, no. 6, pp. 1297–1300, 2017.
[8] C. Sgraja and J. Lindner, "Estimation of rapid time-variant channels for OFDM using Wiener filtering," in *IEEE International Conference on Communications (ICC)*, vol. 4, May 2003, pp. 2390–2395 vol.4.
[9] C. Shin, J. Andrews, and E. Powers, "An efficient design of doubly selective channel estimation for OFDM systems," *IEEE Trans. Wireless Commun.*, vol. 6, no. 10, pp. 3790–3802, October 2007.
[10] V. Savaux and F. Bader, "Mean square error analysis and linear minimum mean square error application for preamble-based channel estimation in orthogonal frequency division multiplexing/offset quadrature amplitude modulation systems," *IET Communications*, vol. 9, no. 14, 2015.
[11] Z. Tang, R. C. Cannizzaro, G. Leus, and P. Banelli, "Pilot-assisted time-varying channel estimation for OFDM systems," *IEEE Transactions on Signal Processing*, vol. 55, no. 5, pp. 2226–2238, 2007.
[12] F. Hlawatsch and G. Matz, *Wireless communications over rapidly time-varying channels*. Academic Press, 2011.
[13] G. B. Giannakis and C. Tepedelenlioglu, "Basis expansion models and diversity techniques for blind identification and equalization of time-varying channels," *Proc. IEEE*, vol. 86, no. 10, pp. 1969–1986, 1998.
[14] D. K. Borah and B. Hart, "Frequency-selective fading channel estimation with a polynomial time-varying channel model," *IEEE Transactions on Communications*, vol. 47, no. 6, pp. 862–873, 1999.
[15] T. Zemen and C. F. Mecklenbräuker, "Time-variant channel estimation using discrete prolate spheroidal sequences," *IEEE Transactions on signal processing*, vol. 53, no. 9, pp. 3597–3607, 2005.
[16] W.-G. Song and J.-T. Lim, "Pilot-symbol aided channel estimation for OFDM with fast fading channels," *IEEE Transactions on Broadcasting*, vol. 49, no. 4, pp. 398–402, 2003.
[17] R. Nissel and M. Rupp, "Doubly-selective MMSE channel estimation and ICI mitigation for OFDM systems," in *IEEE International Conference on Communications (ICC)*, June 2015.
[18] R. Nissel, M. Lerch, M. Šimko, and M. Rupp, "Bit error probability for pilot-symbol-aided OFDM channel estimation in doubly-selective channels," in *International ITG WSA*, Mar 2014.
[19] R. Nissel, S. Caban, and M. Rupp, "Closed-Form capacity expression for low complexity BICM with uniform inputs," in *IEEE PIMRC*, Aug 2015, pp. 678–682.
[20] M. Fuhrwerk, S. Moghaddamnia, and J. Peissig, "Scattered pilot-based channel estimation for channel adaptive FBMC-OQAM systems," *IEEE Trans. Wireless Commun.*, vol. 16, no. 3, pp. 1687–1702, March 2017.
[21] R. Nissel and M. Rupp, "On pilot-symbol aided channel estimation in FBMC-OQAM," in *IEEE International Conference on Acoustics, Speech and Signal Processing (ICASSP)*, March 2016, pp. 3681–3685.
[22] R. Nissel, S. Caban, and M. Rupp, "Experimental evaluation of FBMC-OQAM channel estimation based on multiple auxiliary symbols," in *IEEE SAM*, July 2016.
[23] R. Nissel and M. Rupp, "Bit error probability for pilot-symbol aided channel estimation in FBMC-OQAM," in *IEEE ICC*, May 2016.
[24] T. T. Nguyen, S. T. Le, R. Nissel, M. Wuilpart, L. Van Compernolle, and P. Mégret, "Pseudo-pilot coding based phase noise estimation for coherent optical FBMC-OQAM transmissions," *Journal of Lightwave Technology*, vol. 36, no. 14, pp. 2859–2867, 2018.
[25] R. Nissel, E. Zöchmann, and M. Rupp, "On the influence of doubly-selectivity in pilot-aided channel estimation for FBMC-OQAM," in *IEEE Vehicular Technology Conference (VTC Spring)*, June 2017.
[26] M. Saideh, M. Berbineau, and I. Dayoub, "On the performance of sliding window TD-LMMSE channel estimation for 5G waveforms in high mobility scenario," *IEEE Trans. Veh. Technol.*, 2018, to appear.
[27] R. Nissel, M. Lerch, and M. Rupp, "Experimental validation of the OFDM bit error probability for a moving receive antenna," in *IEEE Vehicular Technology Conference (VTC)*, Sept 2014.
[28] S. Caban, R. Nissel, M. Lerch, and M. Rupp, "Controlled OFDM measurements at extreme velocities," in *Extreme Conference on Communication and Computing (ExtremeCom 2014)*, 2014.
[29] F. Rottenberg, X. Mestre, D. Petrov, F. Horlin, and J. Louveaux, "Parallel equalization structure for MIMO FBMC-OQAM systems under strong time and frequency selectivity," *IEEE Transactions on Signal Processing*, vol. 65, no. 17, pp. 4454–4467, Sept 2017.
[30] A. A. Nagy and S. Weiss, "Channel equalisation of a MIMO FBMC/OQAM system using a polynomial matrix pseudo-inverse," in *IEEE SAM*, 2018.
[31] R. Nissel, M. Rupp, and R. Marsalek, "FBMC-OQAM in doubly-selective channels: A new perspective on MMSE equalization," in *IEEE SPAWC*, July 2017.